Journal of Power Sources 185 (2008) 1575–1579

Contents lists available at ScienceDirect

Journal of Power Sources

journal homepage: www.elsevier.com/locate/jpowsour

Short communication

Safe, high-energy supercapacitors based on solvent-free ionic liquid electrolytes

Catia Arbizzani, Maurizio Biso[1], Dario Cericola[2], Mariachiara Lazzari, Francesca Soavi, Marina Mastragostino*

University of Bologna, Dipartimento di Scienza dei Metalli, Elettrochimica e Tecniche Chimiche, via S. Donato 15, 40127 Bologna, Italy

ARTICLE INFO

Article history:
Received 5 August 2008
Received in revised form 8 September 2008
Accepted 10 September 2008
Available online 19 September 2008

Keywords:
Ionic liquid
Double-layer supercapacitor
Hybrid supercapacitor
Activated carbon
Poly(3-methylthiophene)
Power-assisted HEV

ABSTRACT

Safety is the main concern for energy storage-system application in hybrid-electrical vehicles (HEVs) and ionic liquids (ILs) of low vapor pressure and high thermal stability represent a strategy to meet this key requisite. The use of solvent-free ILs in supercapacitors enables the high cell voltages required for increasing supercapacitor energy up to the values for power-assist application in HEVs. In order to exploit the wide electrochemical stability window of ILs, tailored electrode materials and cell configurations have to be used. The performance of asymmetric double-layer carbon supercapacitors (AEDLCs) and carbon/poly(3-methylthiophene) hybrid supercapacitors operating with different pyrrolidinium-based ILs are reported and compared. This study demonstrates that a design-optimized AEDLC operating with safe, solvent-free IL electrolyte meets cycling stability and the energy and power requisites for power-assisted HEVs at the investigated temperatures.

1. Introduction

The high specific power and very long cycle life make electrochemical double-layer carbon supercapacitors (EDLCs) key energy storage systems for sustainable transport based on hybrid electric vehicles (HEVs) [1–4]. Compared to batteries, supercapacitors feature significantly lower specific energy, i.e. 5 Wh kg^{-1} at maximum, so that even the best performing ones do not yet fulfill the specific energy requisites for power assist in strong-HEV. This application requires that a significant portion of the driveline power is electric and the targets of the electrochemical energy storage systems stated by the United States Advanced Battery Consortium (USABC) and the Department of Energy (DOE) are pulse power of 620 W kg^{-1} for 10 s over more than 3×10^5 shallow cycles and 7.5 Wh kg^{-1} total available energy. These requirements should be in the −30 °C/+60 °C duty temperature range, with safety being a primary target [3,4]. While recent advances in Li-ion batteries have raised their power performance up to target levels, serious concerns still remain about reliability and safety because of their low tolerance to such abusive conditions as overcharge and exposure to high temperatures. The EDLCs feature positive and negative electrodes identical in mass and composition and are charged/discharged by physical processes so that they are intrinsically safer than batteries. Furthermore, unlike batteries, the energy efficiency of EDLCs is higher than 90% so that the amount of released heat is small and can be easily dissipated [1,2]. Thus, supercapacitors of increased energy with respect to commercial ones could compete with Li-ion batteries in power-assisted HEVs, with the advantage of higher safety and reliability than the latter.

Given that the maximum energy (E_{max}) of the supercapacitor is directly related to its capacitance (C_{sc}) and to the square of the maximum operating voltage (V_{max}), as in Eq. (1)

$$E_{max} = \frac{3}{8} C_{sc} V_{max}^2, \quad (1)$$

when delivered between V_{max} and $1/2V_{max}$, the challenge in the supercapacitor field is to develop materials and configurations that make it possible to increase C_{sc} and V_{max}. The most powerful strategy for increasing supercapacitor energy is to raise the cell voltage above 2.5 V/2.7 V, the highest values for commercial systems based on organic electrolytes, without sacrificing cycle-life and safety. Much attention has thus been focused on ionic liquids (ILs) that feature high thermal and chemical stability, low vapor pressure, a wider electrochemical stability window (ESW) than conventional organic electrolytes' and are able to operate in high temperature

* Corresponding author. Tel.: +39 051 2099798; fax: +39 051 2099365.
E-mail address: marina.mastragostino@unibo.it (M. Mastragostino).
[1] Present address: Italian Institute of Technology, Via Morego 30, 16163 Genova, Italy.
[2] Present address: Paul Scherrer Institut, 5232 Villigen PSI, Switzerland.

0378-7753/$ – see front matter © 2008 Elsevier B.V. All rights reserved.
doi:10.1016/j.jpowsour.2008.09.016

regimes that are not feasible with commercial systems [5–11]. The challenge is to design solvent-free IL electrolytes that match these properties with conductivity at least as high as 10^{-3} S cm^{-1} to 10^{-1} S cm^{-1} in a wide-duty temperature range from ca. −30 °C to 60 °C. The high conductivity requisite is crucial for a low equivalent series resistance (ESR), which in turn affects supercapacitor power performance as per the maximum specific power P_{max} in Eq. (2)

$$P_{max} = \frac{V_{max}^2}{4\ ESR\ w_{sc}}, \quad (2)$$

where w_{sc} is the total composite electrode loading.

The most widely studied ILs for supercapacitor application are imidazolium and pyrrolidinium salts; while the former typically display the highest conductivities, the latter feature the widest ESWs, even exceeding 5 V. Table 1 reports conductivity, ESW, melting temperature, which is the limit for the use of ILs as solvent-free electrolytes, formula weight and density of N-butyl-N-methyl pyrrolidinium (PYR_{14}^+)- and N-methoxyethyl-N-methylpyrrolidinium ($PYR_{1(2O1)}^+$)-based ILs with bis(trifluoromethanesulfonyl)imide ($TFSI^-$) and trifluoromethanesulfonate (Tf^-) anions [5,11–16]. The PYR_{14}^+-based ILs freeze near 0 °C and the introduction of a methoxyethyl group on the nitrogen atom of the pyrrolidinium ring in $PYR_{1(2O1)}$TFSI lowers the freezing point to −95 °C and improve the conductivity properties, making this IL one of the most promising for the development of high voltage supercapacitors operating in a wide temperature range.

ILs require the use of specifically designed electrode materials, especially in regard to the electrode/IL interface properties and tailored supercapacitor configurations to take full advantage of their wide ESW. EDLCs with positive and negative carbon electrodes of equal mass, hereinafter termed symmetric EDLCs, do not feature the high V_{max} enabled by ILs because the potential of discharged carbon electrodes is generally far from the mid-point of the IL's ESW and upon charge the two electrodes experience the same potential excursion, so that V_{max} is constrained by the electrode that first hits the ESW limit. Indeed, despite the IL's wide ESW, symmetric EDLCs with PYR_{14}TFSI electrolyte cannot be cycled with coulombic efficiency >95%, which is a requisite for long cycle-life, when V_{max} is ≥3.5 V [9,11]. In IL-based EDLCs with different loadings of the same carbon at the positive and negative electrodes, here termed asymmetric EDLCs (AEDLCs), each electrode can experience different potential excursions and be charged up to the ESW limits of the electrolyte so that V_{max} values 1 V higher than those of commercial, symmetric EDLCs are feasible [10].

A further increase in specific energy with respect to IL-based AEDLCs might be achieved using pseudocapacitive electrode materials coupled to double-layer carbon electrodes in hybrid configurations (HYSC). Pseudocapacitive electrodes of specific capacitance significantly higher than carbons' and that can be charged/discharged several thousand times in aprotic IL by redox processes at potentials approaching the ESW limits should increase the capacitance performance of supercapacitors without sacrificing V_{max} and cycle-life. This is the case of poly(3-methylthiophene) (pMeT), which can be reversibly p-doped/undoped in pyrrolidinium-based ILs at suitably high electrode potentials with specific capacitance of 200–250 F g^{-1} when prepared in IL [18–20].

We report the results of a study designed to develop safe, high-energy AEDLCs and HYSCs based on PYR_{14}TFSI, PYR_{14}Tf and $PYR_{1(2O1)}$TFSI ILs for power-assisted HEV application. The performance at different temperatures of these IL-based AEDLCs and HYSCs with specifically designed carbon and pMeT electrodes is reported and discussed.

2. Experimental

The carbon used in AEDLC and HYSC supercapacitor was PICACTIF SUPERCAP BP10 (Pica) treated at 1050 °C in Ar for 2 h. This surface cleaning procedure was checked by thermogravimetric analysis (TGA) with a Mettler Toledo TGA/SDTA A851 System in the temperature range of 25–1050 °C under N_2 flow at a scanning rate of 20 °C min^{-1}.

Carbon porosity was evaluated by nitrogen adsorption porosimetry carried out at 77 K with an ASAP 2020 system (Micromeritics); the carbon powders were dried for at least 2 h at 120 °C before testing. The N_2 adsorption isotherms were analyzed by the Density Functional Theory (DFT) and the total pore volume (V_{tot}) was evaluated by the quantity of N_2 adsorbed at $p/p^\circ = 0.995$. The carbon electrodes (0.62 cm^2 geometric area) were prepared by mixing 95% (w/w) carbon and 5% (w/w) polytetrafluoroethylene binder (Du-Pont) to yield a paste that was then laminated on carbon-coated aluminum grids (Lamart Corp.).

The PYR_{14}Tf (99%, Solvionic), PYR_{14}TFSI (purum 98%, Solvent Innovation), $PYR_{1(2O1)}$TFSI (Evonik Industries) were dried over night at 80 °C under dynamic vacuum (Büchi Glass Oven B-580) before use; water content in IL was checked by Karl Fisher titration (684 KF Coulometer Metrohm).

The polymer electrodes for the HYSC supercapacitors were obtained by direct electropolymerization of pMeT in IL on a carbon paper aerogel current collector (Marketech). The polymerization bath was 1-ethyl-3-methyl-imidazolium bis(trifluoromethanesulfonyl)imide (EMITFSI, 99%, Solvent Innovation, dried before use)—1 M methylthiophene (Aldrich, distilled before use) with 0.1 M acid additive trifluoromethanesulfonimide (95%, Aldrich) which prevents consumption of the EMITFSI IL at the counter electrode. The polymer was grown by galvanostatic technique at RT and 5 mA cm^{-2} [ref. 18].

"Three-electrode" Swagelok cells were used for single-electrode and supercapacitor tests. For single-electrode studies, double-layer carbon counter-electrode with charge storage capability significantly higher than that of the working electrode was used so as not to limit the capacitive response of the latter. The reference electrode for cyclic voltammetries and for the evaluation of the electrode potentials during supercapacitor galvanostatic cycling was a silver disk; hereinafter the electrode potentials are given vs. the reversible redox couple ferrocene/ferrocinium (Fc/Fc^+, $E_{Fc/Fc^+} = E_{Ag} + 0.200 \pm 0.010$ V). The cells were assembled in dry box (MBraun Labmaster 130, H_2O and O_2 <1 ppm) using a fiberglass separator (Durieux, 200 μm thick when pressed). AEDLCs and HYSC supercapacitors featured w_{sc} of 15–20 mg cm^{-2} and 8 mg cm^{-2}, respectively. The electrochemical tests were performed with a PerkinElmer VMP multichannel potentiostat/galvanostat at temperatures controlled by a Thermoblock (FALC) or a cryostat (HAAKE K40).

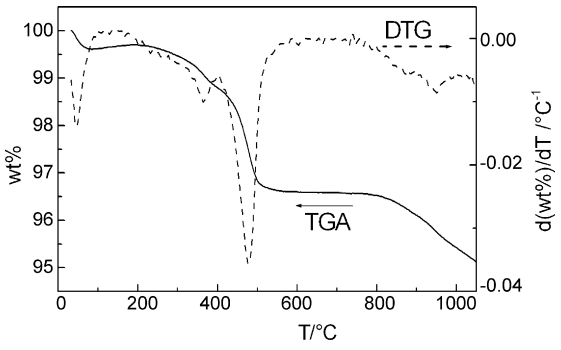

Fig. 1. TGA plot (solid line) and its differential (DTG, dashed line) of the pristine carbon.

Table 1
Conductivity (σ), ESW (evaluated with glassy carbon electrode), melting temperature (T_m), formula weight and density of ILs investigated for supercapacitor applications [5,11–16].

IL	σ (mS cm^{-1})		T_m (°C)	ESW at 60 °C (V)	Formula weight (g mol^{-1})	Density (g ml^{-1})
	RT	60 °C				
$PYR_{14}TFSI$	2.6	6.0	−3	5.5	422	1.41
$PYR_{14}Tf$	2.0	5.5	+3	6.0	291	1.28
$PYR_{1(201)}TFSI$	3.8	8.4	<−90	5.0	424	1.43

3. Results and discussion

To promote carbon wettability with the electrolyte, the surface of the carbon for our IL-based AEDLC and HYSC supercapacitors was cleaned by heat treatment at 1050 °C in Ar atmosphere before use. The TGA curve in Fig. 1 shows that this treatment was effective for the removal of surface acidic groups, which caused the main weight loss at 300–500 °C [21]. Such hydrophilic moieties can be deleterious not just for hydrophobic IL uptake but also for cycling stability because they are typically responsible for irreversible parasitic faradic processes [17,22].

The treated carbon (ACT) featured a total pore volume of 1.2 cm^3 g^{-1} and pore size distribution centered at 2.7 nm; 71% of pore volume was originated by pores wider than 1.5 nm, i.e. wider than IL ion size, and provided a surface area of 940 m^2 g^{-1} accessible to the electrolyte for the double-layer charging process. The ACT electrodes were tested in $PYR_{14}TFSI$, $PYR_{14}Tf$ and $PYR_{1(201)}TFSI$ ILs by cyclic voltammetry (CV) at 20 mV s^{-1} from the potential of the discharged electrode towards positive and negative potentials in order to evaluate capacitance response in the positive and negative domains and to identify the electrode potential ranges that ensure charge/discharge cycles of high coulombic efficiency. The high surface area of the ACT carbon amplifies the faradic contribution to the voltammetric currents related to IL oxidation and reduction when the potentials that mark the ESW limits are approached. Thus, the potential window within which it is possible to charge/discharge the high surface area carbon electrodes is narrower than the ESW reported in Table 1, which was determined with smooth, glassy carbon electrodes. At 60 °C the ACT carbon can be cycled at high efficiency (≥97%) in the range −2.6 V to +1.6 V vs. Fc/Fc$^+$ in the case of $PYR_{14}TFSI$ and $PYR_{14}Tf$ and −2.4 V to +1.6 V vs. Fc/Fc$^+$ in the case of $PYR_{1(201)}TFSI$. In these conditions the ACT carbon featured a specific capacitance of ca. 100 F g^{-1} in all the ILs, a value that decreased by ca. 20% when the temperature was lowered to RT. Given that the potential of the discharged carbon electrode is ca. −0.1 V vs. Fc/Fc$^+$, the negative electrode can sweep a 30% wider potential than the positive during the charge process, and, since the capacitance response is almost the same in the positive and negative domains, it has a higher charge storage capability than the positive. Thus, a proper electrode mass balancing requires 30% more carbon at the positive electrode so as to attain $V_{max} \geq 3.9$ V.

The AEDLC-A, AEDLC-B, and AEDLC-C supercapacitors were assembled with $PYR_{14}TFSI$, $PYR_{14}Tf$ and $PYR_{1(201)}TFSI$ solvent-free ILs, respectively, and ACT carbon electrodes with positive to negative electrode loading ratio (w_+/w_-) higher than 1 (Table 2). The AEDLCs were tested at 60 °C over several thousand galvanostatic charge/discharge cycles (>20,000 cycles) at 10–20 mA cm^{-2}, with $V_{max} > 3.5$ V and mainly ranging between 3.7 V and 4.0 V. The efficacy of the asymmetric configuration is demonstrated in Fig. 2, which shows the charge/discharge galvanostatic profiles of the AEDLC-C supercapacitor (left axis) with $PYR_{1(201)}TFSI$ electrolyte upon the 17,000th charge/discharge cycle at 10 mA cm^{-2} and 60 °C with $V_{max} = 3.8$ V and of its positive and negative electrodes (right axis) which reached the end-of-charge potentials of 1.6 V vs. Fc/Fc$^+$ and −2.2 V vs. Fc/Fc$^+$, respectively. The end-of-discharge potential of the two electrodes is higher than that at the first cycles (ca. −0.1 V vs. Fc/Fc$^+$) because of cell equilibration upon cycling. Table 2 reports the C_{sc}, ESR, E_{max} (from V_{max} to $1/2V_{max}$) and P_{max} values evaluated from discharge cycles carried out at 20 mA cm^{-2} and 60 °C with the reported V_{max} of the AEDLCs assembled with the different ILs. Given that it is feasible to assume that w_{sc} will be one-third of the supercapacitor module weight (w_{module}), the E_{max} values in Table 2 become 10–12 Wh kg^{-1}, i.e. double that of the EDLCs on the market at RT, whose cycling performance decreases as temperature increaes. This high-energy performance of IL-based AEDLCs was exhibited without sacrificing power and cyclability, the latter being tested by deep discharge cycles from V_{max} down to 0 V at 60 °C. The highest cycling stability was exhibited by the $PYR_{1(201)}TFSI$-based AEDLC-C, with a capacitance fade of 2% over 27,000 cycles performed with $V_{max} \leq 3.6$ V for the first 12,000 cycles and 3.7 V for the following 15,000 (3000 cycles were also carried out with $V_{max} = 3.8$ V), as

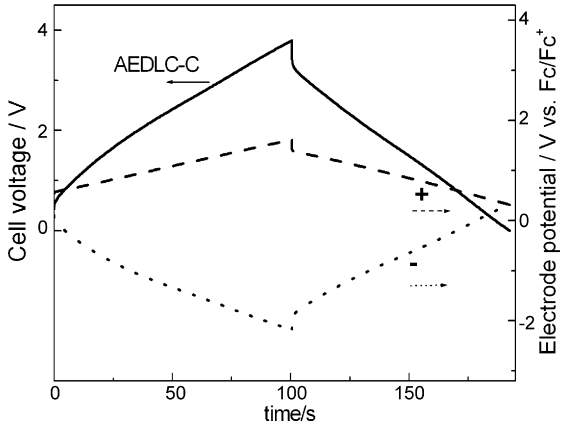

Fig. 2. Voltage profiles of the AEDLC-C supercapacitor with $PYR_{1(201)}TFSI$ electrolyte upon the 17,000th galvanostatic charge/discharge cycle at 10 mA cm^{-2} and 60 °C with $V_{max} = 3.8$ V and of its positive and negative ACT electrodes.

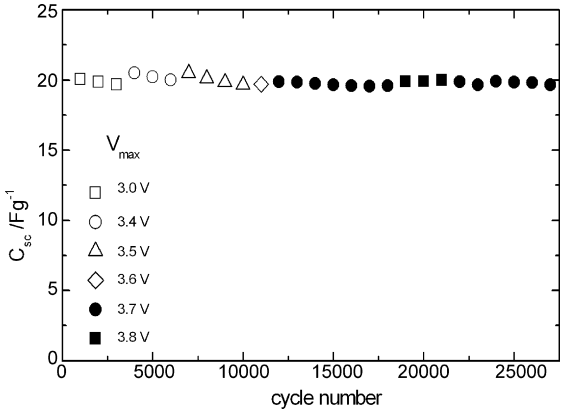

Fig. 3. Trend of specific capacitance (C_{sc}, in F g^{-1} of total composite electrode materials) over cycling at 60 °C and 20 mA cm^{-2} at different V_{max} of the AEDLC-C supercapacitor with $PYR_{1(201)}TFSI$ electrolyte.

Table 2
Positive to negative electrode loading ratio (w_+/w_-) of the AEDLC and HYSC supercapacitors with different ILs, and values of C_{sc}, ESR, E_{max} (delivered from V_{max} to $1/2V_{max}$) and P_{max} evaluated from galvanostatic cycles at ca. 1 A g^{-1} and 60 °C with the reported maximum cell voltage (V_{max}); specific values calculated considering only total composite electrode weight (w_{sc}).

Supercapacitor configuration	CODE	IL	w_+/w_-	V_{max} (V)	C_{sc} (F g^{-1})	ESR (Ω cm^2)	E_{max} (Wh kg^{-1})	P_{max} (kW kg^{-1})
Asymmetric EDLC	AEDLC-A	$PYR_{14}TFSI$	1.34	4.0	22	24	37	9.3
	AEDLC-B	$PYR_{14}Tf$	1.49	4.0	24	25	40	9.1
	AEDLC-C	$PYR_{1(2O1)}TFSI$	1.49	3.7	22	20	31	9.9
Hybrid supercapacitor	HYSC-A	$PYR_{14}TFSI$	0.74	3.9	32	35	51	13

shown by the C_{sc} trend vs. cycle number in Fig. 3. The AEDLC-A with $PYR_{14}TFSI$ featured 20% capacitance fade over 26,000 cycles with V_{max} between 3.6 V and 4.0 V, the last 20,000 being performed at the highest potential. The capacitance of the AEDLC-B supercapacitor with $PYR_{14}Tf$ decreased by 35% after 20,000 cycles, which were performed with V_{max} of 3.5 V/3.9 V over the first 8000 cycles and of 4.0 V in the following 12,000. The lower stability of the latter supercapacitor was mainly due to the fact that the hydrophilic character of $PYR_{14}Tf$ made it impossible to lower the water content in the electrolyte below 100 ppm with our drying procedure. On the other hand the dried, hydrophobic $PYR_{14}TFSI$ and $PYR_{1(2O1)}TFSI$ ILs featured ≤20 ppm of water. Thus, despite the higher formula weight of $PYR_{14}TFSI$ and $PYR_{1(2O1)}TFSI$ with respect to $PYR_{14}Tf$, which may eat into module gravimetric performance, we focused the following tests on the AEDLC-A and AEDLC-C systems. For a better comparison with practical performance of supercapacitors, average specific energy (E) and power (P) values were calculated from galvanostatic discharge curves at different current densities between V_{max}, and 1.35 V and at 60 °C and 20 °C using Eqs. (3) and (4):

$$E = i \int_{t_{V_{max}}}^{t_{1.35\,V}} \frac{V\,dt}{w_{module}} \quad (3)$$

$$P = \frac{E}{t_{1.35\,V} - t_{V_{max}}}, \quad (4)$$

respectively, where i is the current density, $t_{V_{max}}$ and $t_{1.35\,V}$ are the times at which the cells exhibit V_{max} and 1.35 V potentials and $w_{module} = 3w_{sc}$ is the expected weight of a complete supercapacitor module, including case. In Eqs. (3) and (4), 1.35 V was taken as end-discharge potential because it corresponds to that of the best performing EDLCs on the market, which operate between V_{max} and $1/2V_{max}$ with V_{max} = 2.7 V. The average E and P values of the AEDLC-A and AEDLC-C supercapacitors cycled with V_{max} of 3.9 V and 3.7 V, respectively, are shown in the Ragone plots in Fig. 4; the figure also highlights the requirement for power-assisted HEV application of electrochemical energy storage systems [3,4]. The 7.5 Wh kg^{-1} and 660 W kg^{-1} USABC target is met, and even exceeded, at 60 °C by both the AEDLCs and down to 20 °C only by the AEDLC-C with discharges at 10–20 mA cm^{-2} (0.5–1.0 A g^{-1}) from the fully charged state to 1.35 V, which corresponds to a D.O.D. of ca. 50%, as evaluated on the basis of practical charge values at the given rates. When the temperature is lowered from 60 °C to 20 °C, at i > 20 mA cm^{-2} the average specific energies of the AEDLCs decrease mainly because of the increase in the ohmic drop, that lowers the effective maximum cell voltage at which cell discharge begins. Because of the higher conductivity of $PYR_{1(2O1)}TFSI$ than $PYR_{14}TFSI$, the ohmic drop in the AEDLC-C is lower than in the AEDLC-A. Thus, despite the higher V_{max} of the latter, the former features higher practical energy and power values at both temperatures and has the extra advantage of being able to operate below RT because of the low freezing point of $PYR_{1(2O1)}TFSI$. These results were obtained with home-made cells; automated assembly and using a thinner separator than that featured by the AEDLCs would positively affect ohmic drop and E and P values.

To achieve higher specific energy than that of the IL-based AEDLCs, the $PYR_{14}TFSI$-based HYSC-A hybrid system was assembled with the same ACT carbon at the negative electrode and pMeT electropolymerized in IL as positive. We have already demonstrated that this electropolymerization enables pMeT electrodes to deliver specific capacitance of up to ca. 200 F g^{-1} in IL, i.e. double that of the double-layer carbons, in the potential range +0.3 V to +1.3 V vs. Fc/Fc$^+$ [18,19]. The HYSC-A cell was assembled with positive and

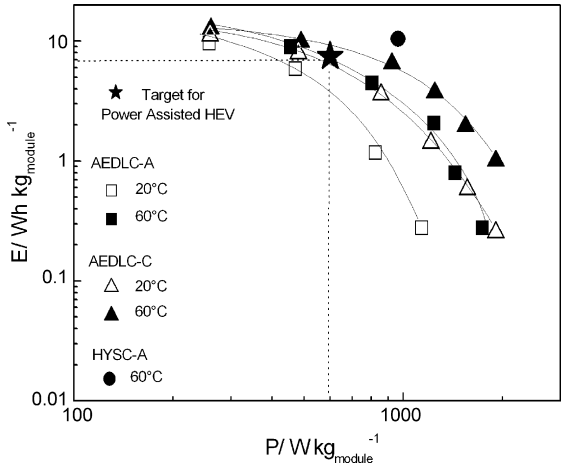

Fig. 4. Average specific energy (E) and power (P) values referred to expected module weight of IL-based AEDLC-A, AEDLC-C and HYSC-A supercapacitors from galvanostatic discharge curves at different currents and 20 °C and 60 °C between V_{max} and 1.35 V. For AEDLC-A, AEDLC-C and HYSC-A the V_{max} was 3.9 V, 3.7 V and 3.9 V, respectively; the currents were 5 mA cm^{-2}, 10 mA cm^{-2}, 20 mA cm^{-2}, 30 mA cm^{-2}, 40 mA cm^{-2}, 50 mA cm^{-2} for the AEDLCs (for AEDLC-A the data at 20 °C with i = 40 mA cm^{-2} and 50 mA cm^{-2} are not included) and 10 mA cm^{-2} for HYSC-A.

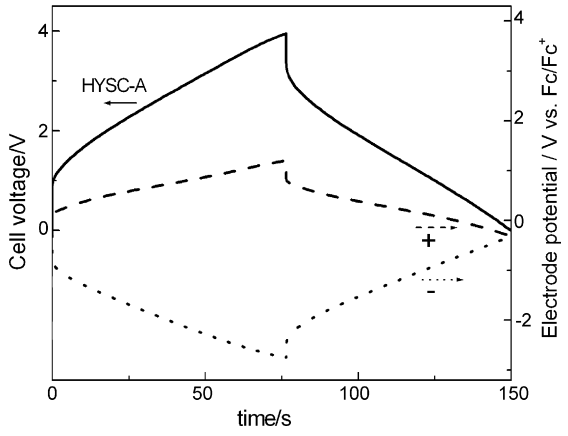

Fig. 5. Voltage profiles of the HYSC-A supercapacitor with $PYR_{14}TFSI$ electrolyte upon galvanostatic charge/discharge at 10 mA cm^{-2} and 60 °C with V_{max} = 3.9 V and of its pMeT positive and ACT negative electrodes.

negative electrodes with mass loading balanced on the basis of each charge storage capability, which in turn depends on specific capacitance and on the widest potential range for the electrode charge process. Table 2 shows the cycling performance at 60 °C of the HYSC-A, which was assembled with a w_+/w_- ratio <1 for a V_{max} of 3.9 V. The data were calculated from the galvanostatic profile at 10 mA cm^{-2} in Fig. 5, which also shows the potentials of the positive and negative electrodes of the HYSC-A system. The use of the pMeT electrode provides a 50% increase of C_{sc} and E_{max} with respect to those of the AEDLCs, i.e. 32 F g^{-1} and 51 Wh kg^{-1} are reached without sacrificing power; the expected E_{max} values of a complete module becomes at least 15 Wh kg^{-1}. The excellent performance of HYSC-A is highlighted in Fig. 4: the average values of E and P at 10 mA cm^{-2} and 60 °C for a hybrid supercapacitor module exceed the requirements for power-assisted HEVs. Note, however, that its cycling stability was not sufficiently long (data not reported). The HYSC-A's specific capacitance halved after 5000 cycles due to deterioration of the polymer electrode. Upon cycling, the positive electrode resistance markedly increased, presumably because pMeT swelling by IL worsened the electronic interchain conductivity in the polymer.

4. Conclusions

This is the first time that the performance at 60 °C and 20 °C of supercapacitors with different solvent-free ILs and featuring AEDLC and HYSC configurations are reported and compared for power-assisted HEV application. We demonstrate that pyrrolidinium-based AEDLCs meet, and even exceed at the highest temperature, the energy and power targets for this application, with cyclability over more than 20,000 cycles at 60 °C. Such asymmetric double-layer supercapacitors reach V_{max} of 4.0 V and E_{max} approaching 40 Wh kg^{-1} (only electrode materials included) so that they can compete with batteries and have the added advantage of inherently higher safety. While an IL-based hybrid supercapacitor with pMeT positive electrode electropolymerized in IL, negative carbon electrode and $PYR_{14}TFSI$ electrolyte delivers 30% higher energy than the AEDLCs, its cycling stability is not high enough to compete with the latter systems.

Acknowledgements

Work funded by the European Commission in the Sixth Framework Programme, Sub-programme Sustainable Surface Transport, under Contract No. TST4-CT-2005-518307 (Project ILHYPOS "Ionic Liquid-based Hybrid Supercapacitor"). All the partners in the Project are acknowledged. Evonik Industries provided $PYR_{1(2O1)}TFSI$.

References

[1] J.R. Miller, A.F. Burke, Interface 17 (2008) 53–57.
[2] A.F. Burke, Electrochim. Acta 53 (2007) 1083–1091.
[3] D. Howell, Energy Storage Research and Development, Vehicle Technology Program, 2007 Annual Progress Report, U.S. Department of Energy, Office of Vehicle Technologies Washington, DC, 2007, available at http://www1.eere.energy.gov/vehiclesandfuels/pdfs/program/2007_energy_storage.pdf.
[4] S.G. Stewart, V. Srinivasan, J. Newman, J. Electrochem. Soc. 155 (2008) A664–A671.
[5] M. Galiński, A. Lewandowski, I. Stępniak, Electrochim. Acta 51 (2006) 5567–5580.
[6] A. Lewandowski, M. Galinski, J. Power Sources 173 (2007) 822–828.
[7] M. Mastragostino, F. Soavi, J. Power Sources 174 (2007) 89–93.
[8] H. Liu, G. Zhu, J. Power Sources 171 (2007) 1054–1061.
[9] A. Balducci, R. Dugas, P.L. Taberna, P. Simon, D. Plée, M. Mastragostino, S. Passerini, J. Power Sources 165 (2007) 922–927.
[10] M. Lazzari, F. Soavi, M. Mastragostino, J. Power Sources 178 (2008) 490–496.
[11] M. Mastragostino, F. Soavi, in: J. Garche, C.K. Dyer, P. Moseley, Z. Ogumi, D. Rand, B. Scrosati (Eds.), Encyclopedia of Electrochemical Power Sources, Elsevier B.V., in press.
[12] S. Zhang, N. Sun, X. He, X. Lu, X. Zhang, J. Phys. Chem. Ref. Data 35 (2006) 1475–1517.
[13] Z.-B. Zhou, H. Matsumoto, K. Tatsumi, Chem. Eur. J. 12 (2006) 2196–2212.
[14] W.A. Henderson, S. Passerini, Chem. Mater. 16 (2004) 2881–2885.
[15] M. Conte, 23rd International Electric Vehicle Symposium (EVS23), Anaheim, CA, December 2–5, 2007.
[16] D. Cericola, Graduate Thesis, University of Bologna, Italy, October 2007.
[17] M. Lazzari, M. Mastragostino, F. Soavi, Electrochem. Commun. 9 (2007) 1567–1572.
[18] C. Arbizzani, S. Beninati, M. Lazzari, F. Soavi, M. Mastragostino, J. Power Sources 174 (2007) 648–652.
[19] M. Biso, M. Mastragostino, M. Montanino, S. Passerini, F. Soavi, Electrochim. Acta 53 (2008) 7967–7971.
[20] D.-W. Kim, S.R. Sivakkumar, D.R. MacFarlane, M. Forsyth, Y.-K. Sun, J. Power Sources 180 (2008) 591–596.
[21] J.L. Figueiredo, M.F.R. Pereira, M.M.A. Freitas, J.J.M. Órfão, Carbon 37 (1999) 1379–1389.
[22] A.G. Pandolfo, A.F. Hollenkamp, J. Power Sources 157 (2006) 11–27.